Nonlinear Dyn (2012) 69:1009–1021
DOI 10.1007/s11071-011-0323-9

ORIGINAL PAPER

Continuous-time bilinear system identification using single experiment with multiple pulses

Jer-Nan Juang · Cheh-Han Lee

Received: 26 March 2010 / Accepted: 28 December 2011 / Published online: 18 January 2012
© Springer Science+Business Media B.V. 2012

Abstract A novel method is presented for the identification of a continuous-time bilinear system from the input–output data generated by a single experiment with multiple pulses. In contrast to the conventional approach utilizing multiple experiments, the current work documents the advantage of using a single experiment and sets up a procedure to obtain bilinear system models. The special pulse inputs employed by earlier research can be avoided and accurate identification of the continuous-time system model is possible by performing a single experiment incorporating a class of control input sequences combining pulses with free-decay response. The algorithm presented herein is more attractive in practice for the identification of bilinear systems. Numerical examples presented demonstrate the methodology developed in the paper.

Keywords Bilinear system identification · Nonlinear system identification · System realization · Experimental dynamical modeling

1 Introduction

Identification of continuous-time systems is a fundamental problem with applications in many disciplines of science. Methods for realizing linear time invariant models of dynamical systems are well understood [1, 2]. However, much work remains to be done for identification of continuous-time bilinear systems which constitute a well structured subclass of nonlinear systems. A class of nonlinear systems can be approximated by a bilinear system to an arbitrary high order as needed. The approximation procedure such as Carleman linearization [3, 4] and Lo's theorem [5] can be used to transform a nonlinear system to a different corresponding bilinear system.

A bilinear system may be described by a linear time invariant model plus a state and control-input coupling term [6–9]. Bilinear models become time invariant when input values are constant. Bilinear differential equations are used to model several physical systems such as the automobile brake dynamics, nuclear reactor dynamics, and certain biological processes [10]. However, in practice it is quite difficult to use these models effectively for estimation and control purposes, owing to the parametric uncertainty associated with the models. Continuous-time bilinear system identification provides a solution to this problem by enabling the determination of bilinear system models directly from experimental data.

In the past few decades, researchers on bilinear system identification focused on the relation of the input–output equation in terms of function series, such as orthogonal series approach [11], Walsh functions [12, 13], block-pulse functions [14, 15], Chebyshev polynomials [16], Legendre polynomials [17],

J.-N. Juang (✉) · C.-H. Lee
National Cheng-Kung University, Tainan 70101, Taiwan
e-mail: jjuang88@gmail.com

Hartley-based modulating functions [18, 19], and Fock functionals [20, 21]. Juang [22] originated a comprehensive solution to this classical problem of bilinear system identification [8, 9]. The drawback of this solution is that it requires multiple experiments starting with the system at rest to formulate enough equations for determination of bilinear system models. It is quite difficult, if not impossible, to use the multiple-experiment method for real-time/on-line applications.

On the other hand, there is also recent work in discrete-time bilinear state-space model identification. Phan and Celik [23] tried to convert the discrete-time bilinear system into an equivalent linear model where the input excitation could be a random signal. Unfortunately, the two types of models (i.e., continuous-time and discrete-time bilinear models) are not equivalent in the sense that there does not exist any definite connection to convert back and forth between them. At the present stage of development, continuous-time bilinear system identification and discrete-time bilinear system identification remain two separate tracks. Nevertheless, bilinear system identification requires some kind of discrete-time model in the parameter-estimation process due to its digital nature of data measurement. Ekman and Larson [24] introduced an integral approach in which the continuous-time bilinear system given in state-space form was approximately transformed via integration operations into a discrete-time regression model. The model parameters in the discrete-time regression model is thereafter estimated using the principle of separable nonlinear least-squares. Note that there is no definite connection between the conventional discrete-time bilinear model and the discrete-time regression model.

In this paper, we develop a method similar to the original one [22] without the requirement of multiple experiments. The Single Experiment with Multiple Pulses (SEMP) method requires only a single experiment using multiple pulses with free-decay in between. Note that a single experiment with a single pulse is insufficient to identify the input/output behavior of bilinear systems [25]. The SEMP method significantly advances the original approach toward the real-time/on-line applications, which is shown as follows.

2 Basic formulation

This section will first describe the continuous-time bilinear system equations together with the simple but efficient observations of using constant input to simplify the system originally introduced by Juang [22]. Then it is followed by a subsection introducing the basic equations used to identify the bilinear system.

2.1 System equations

Let x be the state vector of $n \times 1$, A_c the state matrix of $n \times n$, u the input vector of $r \times 1$, B_c the input matrix of $n \times r$. The bilinear state equation in the continuous-time domain is expressed by

$$\dot{x} = A_c x + \sum_{i=1}^{r} N_{ci} x u_i + B_c u \tag{1}$$

where N_{ci} $(i = 1, 2, \ldots, r)$ is the $n \times n$ weighting matrix of the couple term xu_i between the state vector x and ith input u_i in the input vector u of length r. The bilinear system of (1) can also be formulated by a more compact representation as the following

$$\dot{x} = A_c x + N_c u \otimes x + B_c u \tag{2}$$

where the symbol $\otimes$ means the Kronecker product and

$$N_c = [\, N_{c1} \quad N_{c2} \quad \cdots \quad N_{cr} \,] \tag{3}$$

is the bilinearity matrix of $n \times nr$. The corresponding measurement equation is

$$y = Cx + Du \tag{4}$$

where y is the output measurement vector of $m \times 1$, C is the output matrix of $m \times n$, and D is the direct transmission matrix of $m \times r$.

For a specific constant input $u = w_i$ where i is an arbitrary integer to represent a specific choice for the constant input vector u, the bilinear system of equations (2) becomes

$$\dot{x} = (A_c + N_c w_i \otimes I_n)x + B_c w_i \tag{5}$$

where I_n is identity matrix of $n \times n$. The vector w_i is a constant input vector of $r \times 1$ of the designed $r \times s$ constant pulse input matrix

$$W = [\, w_1 \quad w_2 \quad \cdots \quad w_s \,]. \tag{6}$$

Each quantity $w_i, i = 1, 2, \ldots, s$, represents a pulse vector applied at several designated sampling points to create free decay responses. The matrix W must be of the rank r, obviously $s \geq r$, and it is rich enough so that all the system modes can be excited and observable.

The discrete-time model of the system for $u(k) = w_i$ is

$$x(k+1) = \bar{A}_i x(k) + \bar{b}_i, \quad i = 1, 2, \ldots, s \tag{7}$$

with the measurement equation

$$y(k) = Cx(k) + Du(k) \tag{8}$$

where the quantities $\bar{A}_i$ and $\bar{b}_i$ are determined by

$$\bar{A}_i = e^{(A_c + N_c w_i \otimes I_n)\Delta t}, \tag{9}$$

$$\bar{b}_i = \int_0^{\Delta t} e^{(A_c + N_c w_i \otimes I_n)\tau}\, d\tau\, B_c w_i. \tag{10}$$

The quantity Δt is the sampling time.

If the input signal vanishes, the system of (2) reduces to the simple form

$$\dot{x} = A_c x. \tag{11}$$

Its discrete-time model is

$$x(k+1) = Ax(k) \tag{12}$$

where

$$A = e^{A_c \Delta t} \tag{13}$$

and the corresponding measurement equation is also reduced to

$$y(k) = Cx(k). \tag{14}$$

The continuous bilinear system matrices, A_c, B_c, C, D, and N_c are embedded in the discrete equations (7), (8), (12), and (14). Equations (7) to (14) are used as the basis of the identification procedure to be described.

2.2 Preliminary equations for identification

With the help of (7), (8), (12), and (14), the state response for a pulse over a single time period $(k+1)\Delta t > t \geq k\Delta t$ is

$$\begin{aligned} x(k) &= Ax(k-1), \\ x(k+1) &= \bar{A}_i x(k) + \bar{b}_i, \\ x(k+2) &= Ax(k+1), \\ x(k+3) &= A^2 x(k+1), \\ &\vdots \\ x(k+\ell) &= A^{\ell-1} x(k+1), \end{aligned} \tag{15}$$

along with the measurements equations

$$\begin{aligned} y(k) &= Cx(k) + Du(k), \\ y(k+1) &= Cx(k+1) = C\big(\bar{A}_i x(k) + \bar{b}_i\big), \\ y(k+2) &= CAx(k+1), \\ y(k+3) &= CA^2 x(k+1), \\ &\vdots \\ y(k+\ell) &= CA^{\ell-1} x(k+1) \end{aligned} \tag{16}$$

where ℓ is an integer indicating the data length of the free decay which is large enough for identification of the system and will be defined later. Note that (16) is valid only for a single pulse. When a second pulse is applied at the end of the period, i.e., at $k+\ell$, the last measurement equation for $y(k+\ell)$ becomes the same as the first equation with k replaced by $k+\ell$. For the pulse responses of (15) and (16), it is easy to identify the quantities C, A, $x(k+1)$ and all the states after $x(k+1)$ without the knowledge of $x(k)$.

Let us define the augmented measurement vector as

$$h_k = \begin{bmatrix} y(k) \\ y(k+1) \\ \vdots \\ y(k+\alpha-1) \end{bmatrix} \tag{17}$$

where an integer α is introduced to indicate the length of the vector, then we form the Hankel matrix as

$$\begin{aligned} H_{k+1} &= [\, h_{k+1} \quad h_{k+2} \quad \cdots \quad h_{k+\beta} \,] \\ &= \begin{bmatrix} C \\ CA \\ \vdots \\ CA^{\alpha-1} \end{bmatrix} \\ &\quad \times \big[x(k+1) \quad Ax(k+1) \quad \cdots \quad A^{\beta-1} x(k+1) \big] \end{aligned} \tag{18}$$

where an integer β is introduced to increase the column size. The matrix product on the right-hand side of (18) shows the relationship between the free-decay system Markov parameters and the discrete-time system matrices. Assume that the pair (A, C) is observable such that its corresponding observability matrix has the rank n if we choose α larger than or equal to n where n is the number of states. Similarly, the system is excitable by the state $x(k+1)$ in the sense that the controllability-like matrix $[x(k+1), Ax(k+1), \dots, A^{\beta-1}x(k+1)]$ is of rank n for $\beta \geq n$.

Using the singular value decomposition (SVD) to decompose the Hankel matrix yields

$$H_{k+1} = U_{k+1}\Sigma_{k+1}V_{k+1}^T \tag{19}$$

where Σ_{k+1} of $n \times n$ is a square matrix containing n nonzero singular values. The matrix U_{k+1} is of dimension $\alpha m \times n$ and the matrix V_{k+1} is of dimension $\beta \times n$. The matrix U_{k+1} is related to the system matrices C and A by a choice such that

$$U_{k+1} = \begin{bmatrix} C \\ CA \\ \vdots \\ CA^{\alpha-1} \end{bmatrix}. \tag{20}$$

On the other hand, the matrix $\Sigma_{k+1}V_{k+1}^T$ is related to the state matrix $x(k+1)$ by

$$\Sigma_{k+1}V_{k+1}^T = \begin{bmatrix} x(k+1) & Ax(k+1) & \dots & A^{\beta-1}x(k+1) \end{bmatrix}. \tag{21}$$

Equations (20) and (21) clearly imply that

$$C = \text{the first } m \text{ rows of } U_{k+1} \tag{22}$$

and

$$x(k+1) = \text{the first column of } \Sigma_{k+1}V_{k+1}^T. \tag{23}$$

Now, truncating the last m (number of outputs) rows of U_{k+1} yields

$$U_{k+1\uparrow} = \begin{bmatrix} C \\ CA \\ \vdots \\ CA^{\alpha-2} \end{bmatrix} \tag{24}$$

and, similarly, deleting the first m rows of U_{k+1} gives

$$U_{k+1\downarrow} = \begin{bmatrix} CA \\ CA^2 \\ \vdots \\ CA^{\alpha-1} \end{bmatrix} = U_{k+1\uparrow}A. \tag{25}$$

Equation (25) produces the state matrix A by

$$A = U_{k+1\uparrow}^{\dagger}U_{k+1\downarrow}. \tag{26}$$

For the identified state matrix to have the rank n, both $(\alpha-1)m \times n$ matrices $U_{k+1\uparrow}$ and $U_{k+1\downarrow}$ must also have the rank n. This implies that α must be chosen such that $(\alpha-1)m \geq n$, i.e., $\alpha m \geq m + n$.

The relation between system matrix $(\bar{A}_i, \bar{b}_i)$ and the state $x(k)$ is

$$\begin{aligned} x(k+1) &= \bar{A}_i x(k) + \bar{b}_i \\ &= \text{the first column of } \Sigma_{k+1}V_{k+1}^T \\ &= U_{k+1\uparrow}^{\dagger}h_{k+1\uparrow} \end{aligned} \tag{27}$$

where $h_{k+1\uparrow}$ is formed by truncating the last m rows of h_{k+1} and the last equality is based on the fact that $U_{k+1\uparrow}$ is of full rank n. Finally, if we apply another pulse over the time period $(k+\ell+1)\Delta t > t \geq (k+\ell)\Delta t$, then the initial state for that pulse is given by

$$x(k+\ell) = A^{\ell-1}x(k+1) = A^{\ell-1}U_{k+1\uparrow}^{\dagger}h_{k+1\uparrow}. \tag{28}$$

3 SEMP system identification method

The SEMP method for identifying a continuous-time bilinear system model incorporates a class of control input sequences combining pulses with free-decay in between. The pulse duration is one time step Δt. The first pulse of input w_1 excites the system over the time period

$$(k+1)\Delta t > t \geq k\Delta t; \quad \text{with } k = 0 \quad \text{and} \quad u = w_1. \tag{29}$$

Equations (15) and (16) describe the pulse response and measurements, where the free-decay data length ℓ, denoted by ℓ_0, after the first pulse must be selected such that

$$\ell_0 > \alpha + \beta - 1 \tag{30}$$

in order to form the Hankel matrix H_1 defined in (18). The last measurement $y(\alpha+\beta-1)$ used in forming the Hankel matrix H_1 must be a free decay data, i.e., the second pulse is not allowed to apply at the point $\alpha+\beta-1$, and thus the data length ℓ_0 must be larger than $\alpha+\beta-1$ to avoid the possibility of any force application at the point.

Given the pulse index j, the other pulses are applied over the time period

$$(k+j\ell+1)\Delta t > t \geq (k+j\ell)\Delta t \quad \text{with } k=\ell_0+(i-1)(p+1)\ell \quad \text{and} \quad u=w_i \tag{31}$$

where

$$j=(i-1)(p+1), (i-1)(p+1)+1, \dots, i(p+1)-1; \quad i=1,2,\dots,s. \tag{32}$$

The integer i is the control input vector index of w_i in the matrix W defined in (6) and p is the assumed system order. The free-decay data length ℓ is chosen such that

$$\ell > \alpha - 1 \tag{33}$$

to form the augmented measurement vector $h_{k+1\uparrow}$ defined in (17). The same reason given for (30) applies for (31) that no force is allowed to apply at the point $(k+j(\alpha-1))$ to produce a free decay data $y(k+j(\alpha-1))$ to properly form $h_{k+1\uparrow}$. With the choice of $p=n$ and $s=r$, we need at least a total of $(n+1)r+1$ pulses for the SEMP method to identify the bilinear system.

3.1 Step 1: Identification of C and A_c

The initial step begins with the time index $k=0$ and the first pulse of input vector $u=w_1$ to excite the system. The resulting pulse response is then used to identify the matrices C, A and

$$x(1) = \text{the first column of } \Sigma_1 V_1^T \tag{34}$$

directly from (22), (26), and (27). The continuous-time state matrix is calculated with the help of (13) as

$$Ac = \frac{1}{\Delta t}\log(A), \tag{35}$$

and the state vector at $k=\ell_0$ is estimated by (28) as

$$x(\ell_0) = A^{\ell_0-1}x(1) = A^{\ell_0-1}U_{1\uparrow}^{\dagger}h_{1\uparrow} \tag{36}$$

which will be used as the initial condition for the next step. It is important to note that the same observability matrix $U_{1\uparrow}$ is used to keep the identification results on the same coordinate [22].

3.2 Step 2: Identification of $\bar{A}_i$ and $\bar{b}_i$

The second step starts with shifting the time index k to ℓ_0 and using the same pulse vector w_1 to excite the system at the periods defined in (31) to generate a total of $p+1$ pulse responses between the pulse periods. With the pulse response data available, an application of (27) produces

$$\begin{aligned} &\bar{A}_1 x(k) + \bar{b}_1 = U_{1\uparrow}^{\dagger} h_{k+1\uparrow}, \\ &\bar{A}_1 x(k+\ell) + \bar{b}_1 = U_{1\uparrow}^{\dagger} h_{k+\ell+1\uparrow}, \\ &\vdots \\ &\bar{A}_1 x(k+p\ell) + \bar{b}_1 = U_{1\uparrow}^{\dagger} h_{k+p\ell+1\uparrow} \end{aligned} \tag{37}$$

where $h_{k+1\uparrow}, \dots, h_{k+p\ell+1\uparrow}$ are formed by truncating the last m rows of $h_{k+1}, \dots, h_{k+p\ell+1}$, respectively, defined in (17) containing free-decay response data, $x(k)$ is obtained by (36) in the previous step, and

$$\begin{aligned} x(k+j\ell) &= A^{\ell-1}x\big(k+(j-1)\ell+1\big) \\ &= A^{\ell-1}U_{1\uparrow}^{\dagger}h_{k+(j-1)\ell+1\uparrow}; \quad j=1,2,\dots,p. \end{aligned} \tag{38}$$

Rewrite (37) in matrix form as

$$\begin{bmatrix} \bar{A}_1 & \bar{b}_1 \end{bmatrix} \mathcal{X}_1 = \mathcal{Y}_1 \tag{39}$$

where

$$\begin{aligned} \mathcal{X}_1 &= \begin{bmatrix} x(k) & x(k+\ell) & \dots & x(k+p\ell) \\ 1 & 1 & \dots & 1 \end{bmatrix}, \\ \mathcal{Y}_1 &= \begin{bmatrix} U_{1\uparrow}^{\dagger}h_{k+1\uparrow} & U_{1\uparrow}^{\dagger}h_{k+\ell+1\uparrow} & \dots & U_{1\uparrow}^{\dagger}h_{k+p\ell+1\uparrow} \end{bmatrix}. \end{aligned} \tag{40}$$

The matrices $\bar{A}_1$ and $\bar{b}_1$ can then be determined by

$$\begin{bmatrix} \bar{A}_1 & \bar{b}_1 \end{bmatrix} = \mathcal{Y}_1 \mathcal{X}_1^{\dagger}. \tag{41}$$

Note that the matrix $\mathcal{X}_1$ must have the rank $n+1$ in order to obtain a least-squares solution for $\bar{A}_1$ and $\bar{b}_1$. It implies that the integer p must be equal to or greater than the number of states n, i.e., $p \geq n$. This step is completed by computing the initial condition for the next experimental step using (36) for $j = p + 1$,

$$x\big(k + (p+1)\ell\big) = A^{\ell-1} x(k + p\ell + 1) = A^{\ell-1} U_{1\uparrow}^{\dagger} h_{k+p\ell+1\uparrow}. \tag{42}$$

Now set $k = \ell_0 + (i-1)(p+1)\ell$ and continue the experiment by repeating the above process, i.e., by exciting the system with the other input vector sequence w_i for $i = 2, 3, \ldots, s$, to compute all the discrete-time model parameters $\bar{A}_i$'s and $\bar{b}_i$'s.

3.3 Step 3: Identification of $x(0)$ and D

The initial condition for the experiment can be simply determined by substituting $\bar{A}_1$ and $\bar{b}_1$ into (27) as

$$\begin{aligned} x(0) &= \bar{A}_1^{-1}\big[x(1) - \bar{b}_1\big] \\ &= \bar{A}_1^{-1}\big[\text{the first column of } \big(\Sigma_1 V_1^T\big) - \bar{b}_1\big] \\ &= \bar{A}_1^{-1}\big[U_{1\uparrow}^{\dagger} h_{1\uparrow} - \bar{b}_1\big]. \end{aligned} \tag{43}$$

Collect the measurement equations for all pulses as

$$\begin{aligned} y(0) &= Cx(0) + Du(0), \\ y(\ell_0) &= Cx(\ell_0) + Du(\ell_0), \\ y(\ell_0 + \ell) &= Cx(\ell_0 + \ell) + Du(\ell_0 + \ell), \\ &\vdots \\ y(\ell_0 + n_p\ell) &= Cx(\ell_0 + n_p\ell) + Du(\ell_0 + n_p\ell) \end{aligned} \tag{44}$$

where

$$n_p = s(p+1) - 1. \tag{45}$$

Form a matrix equation for (44) to yield

$$D\mathcal{U} = \mathcal{D} \tag{46}$$

where

$$\mathcal{D} = \big[y(0) - Cx(0) \quad y(\ell_0) - Cx(\ell_0) \quad y(\ell_0 + \ell) - Cx(\ell_0 + \ell) \quad \cdots \quad y(\ell_0 + n_p\ell) - Cx(\ell_0 + n_p\ell)\big] \tag{47}$$

is a matrix of size $m \times [s(p+1)+1]$ and

$$\mathcal{U} = \big[u(0) \quad u(\ell_0) \quad u(\ell_0 + \ell) \quad \ldots \quad u(\ell_0 + n_p\ell)\big] \tag{48}$$

is a matrix of size $r \times [s(p+1)+1]$. From (7) to (10), the input vector u is given by

$$\begin{aligned} &u(0) = w_1, \\ &u\big(\ell_0 + (i-1)(p+1)\ell + j\ell\big) = w_i, \\ &\quad i = 1, 2, \ldots, s; \;\; j = 0, 1, \ldots, p. \end{aligned} \tag{49}$$

The direct transmission matrix can be recovered in the least-squares sense by using (46) to have

$$D = \mathcal{D}\mathcal{U}^{\dagger}. \tag{50}$$

The matrix $\mathcal{U}$ must be of rank r, implying that the integer s is equal to or larger than r, i.e., $s \geq r$.

3.4 Step 4: Identification of N_c and B_c

The last step is to compute the $n \times r$ matrix B_c and the weighting/bilinearity matrix N_c associated with the couple term of the state vector x and the input vector u. Equation (9) which defines $\bar{A}_i$ produces

$$A_c + N_c w_i \otimes I_n = \frac{1}{\Delta t}\log(\bar{A}_i), \quad i = 1, 2, \ldots, s. \tag{51}$$

Collect all the above (51) to form the matrix equation as

$$N_c \mathcal{W} = \mathcal{A} \tag{52}$$

where

$$\mathcal{W} = W \otimes I_n \tag{53}$$

is an $rn \times sn$ matrix and

$$\mathcal{A} = \big[\tfrac{1}{\Delta t}\log(\bar{A}_1) - A_c \quad \tfrac{1}{\Delta t}\log(\bar{A}_2) - A_c \quad \ldots \quad \tfrac{1}{\Delta t}\log(\bar{A}_s) - A_c\big] \tag{54}$$

is an $n \times sn$ matrix. So the bilinearity matrix N_c can be obtained by taking

$$N_c = \mathcal{A}\mathcal{W}^\dagger. \tag{55}$$

Take the conversion from discrete-time to continuous-time of (10) and define

$$b_{ci} \equiv \left[I_n \Delta t + \frac{1}{2!}(A_c + N_c w_i \otimes I_n)(\Delta t)^2 + \frac{1}{3!}(A_c + N_c w_i \otimes I_n)^2(\Delta t)^3 + \cdots \right]^{-1} \bar{b}_i. \tag{56}$$

We form the matrix equation for the continuous-time input matrix B_c as

$$B_c W = \mathcal{B} \tag{57}$$

where

$$\mathcal{B} = [\, b_{c1} \quad b_{c2} \quad \ldots \quad b_{cs} \,] \tag{58}$$

is an $n \times s$ matrix. The continuous-time input matrix B_c can then be obtained by solving

$$B_c = \mathcal{B} W^\dagger. \tag{59}$$

To this end, we have identified all continuous-time system matrices A_c, B_c, N_c, C, and D together with the initial condition $x(0)$ for the bilinear system described by (2) and (4) by the SEMP method.

It is worth mentioning that the SEMP method uses $p+2$ pulses of w_1 and $p+1$ pulses of $w_2, w_3, \ldots, w_s$. The order of these pulses is arbitrary so that one of the pulses denoted as w_1 is used $p+2$ times to excite the bilinear system with free-decay response in between to obtain the quantities A_c, C, $x(0)$, $\bar{A}_1$, and $\bar{b}_1$, and the other w_i's are used $p+1$ times each for the rest of identification.

4 Numerical example

Two numerical examples are used to illustrate the SEMP method. The first example is the automobile breaking system described by a second-order differential equation. The second example is the induction motor described by a fourth-order differential equation.

4.1 Automobile breaking system

In this subsection, we will identify an automobile dynamics system under the major influence of conventional frictional braking and acceleration. Following the developments of Mohler [10], the friction force of the automobile brake is nearly proportional to the orthogonal force between the rubbing surface and their relative velocity. The breaking force is modeled by

$$f_b = c_b u_1 \dot{x}_1 \tag{60}$$

where $\dot{x}_1$ is the automobile translation velocity, u_1 the brake pedal control force, and c_b a positive constant. Similarly, other frictional forces may be approximated by

$$f_c = c_f \dot{x}_1 \tag{61}$$

where c_f is a positive constant.

Then a summation of inertial force, friction forces, and normalized engine forces u_2 yields the equation of motion

$$\begin{aligned} \dot{x}_1 &= x_2, \\ \dot{x}_2 &= -\frac{c_f}{m} x_2 - \frac{c_b}{m} u_1 x_2 + u_2 \end{aligned} \tag{62}$$

where x_1 is position, x_2 the translation velocity, and m the mass of the automobile. Rewrite (62) in the form of the state equations (2) to produce

$$\begin{aligned} &x = \begin{bmatrix} x_1 \\ x_2 \end{bmatrix}; \qquad A_c = \begin{bmatrix} 0 & 1 \\ 0 & -\frac{c_f}{m} \end{bmatrix}; \qquad B_c = \begin{bmatrix} 0 & 0 \\ 0 & 1 \end{bmatrix}; \\ &N_c = [\, N_{c1} \quad N_{c2} \,] = \begin{bmatrix} 0 & 0 & 0 & 0 \\ 0 & -\frac{c_b}{m} & 0 & 0 \end{bmatrix}. \end{aligned} \tag{63}$$

Let the initial condition be $x(0) = [\,1.0\ 1.0\,]^T$, and the parameters c_f and c_b be chosen as $c_f = 2m$ and $c_b = 5m$ where m is the automobile mass. Assume that the position and velocity are measured directly, and so assign

$$C = \begin{bmatrix} 1 & 0 \\ 0 & 1 \end{bmatrix} \tag{64}$$

for the measurement equation (4). Also assume that there exists a direct transmission matrix

$$D = \begin{bmatrix} 0.1 & 0 \\ 0 & 0.1 \end{bmatrix} \tag{65}$$

for the testing purpose.

The control input signal designed for identification is

$$W=\begin{bmatrix}1 & 0\\ 1 & 1\end{bmatrix}. \tag{66}$$

Let $p=\alpha=\beta=3$ together with $\ell_0=5$ and $\ell=2$. The input sequence is shown in Fig. 1, where u_1 and u_2 are the sampled inputs at the specific sampling points, $\tilde{u}_1$ and $\tilde{u}_2$ are the pulse inputs used in the excitation/identification procedure with the sampling time $\Delta t=0.1$. We use both inputs with the pulse magnitude of one for the first 15 steps, whereas only the second input with the pulse magnitude of one is used for the remaining steps. The initial pulse applied at $k=0$ generates five $(\alpha+\beta-1=5)$ free-decay response data. All the remaining pulses applied at $k=6,9,12,\ldots$ produce two $(\alpha-1=2)$ free-decay response data each. The response shown in Fig. 2 for the automobile position shows no sign of response decaying because it represents the distance of a moving vehicle. Nevertheless, Fig. 3 shows a clear sign of velocity decaying during the free-decay periods.

With the pulse response data in hand, the SEMP method is applied to produce the following system matrices

$$\begin{aligned}
\tilde{A}_c &= \begin{bmatrix}0.0145 & -0.5661\\ 0.0517 & -2.0145\end{bmatrix}, \qquad \tilde{B}_c=\begin{bmatrix}-2.8439\times10^{-12} & -0.5605\\ 7.4223\times10^{-12} & 1.0641\end{bmatrix},\\
\tilde{N}_c &= [\tilde{N}_{c1}\quad \tilde{N}_{c2}]=\begin{bmatrix}-0.0667 & 2.5985 & 5.2505\times10^{-14} & -2.0463\times10^{-12}\\ 0.1267 & -4.9333 & 2.5729\times10^{-14} & -1.0214\times10^{-12}\end{bmatrix},\\
\tilde{C} &= \begin{bmatrix}-0.5698 & -0.3001\\ -0.0238 & 0.9272\end{bmatrix}, \qquad \tilde{D}=\begin{bmatrix}0.1 & -1.0217\times10^{-11}\\ 9.8070\times10^{-16} & 0.1\end{bmatrix}.
\end{aligned} \tag{67}$$

These identified matrices are similar to the original matrices given in (63). The similarity may be verified by checking their eigenvalues as

$$\begin{aligned}
\lambda(\tilde{A}_c)-\lambda(A_c) &= \begin{bmatrix}-4.4409\times10^{-16}\\ 1.5543\times10^{-15}\end{bmatrix},\\
\lambda(\tilde{N}_{c1})-\lambda(N_{c1}) &= \begin{bmatrix}0\\ -5.0326\times10^{-11}\end{bmatrix},\\
\lambda(\tilde{N}_{c2})-\lambda(N_{c2}) &= \begin{bmatrix}1.0103\times10^{-15}\\ -9.6991\times10^{-13}\end{bmatrix}
\end{aligned} \tag{68}$$

where $\lambda(\cdot)$ denotes the eigenvalues of matrix $(\cdot)$. The difference between true and identified system eigenvalues shows the accuracy of SEMP method. The sin-

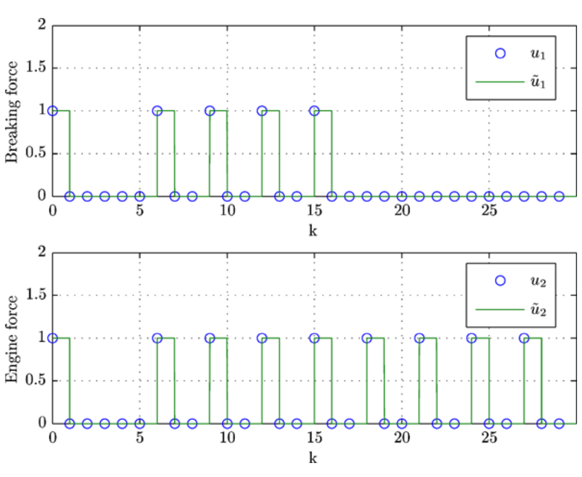

Fig. 1 Sampled and pulse input sequence

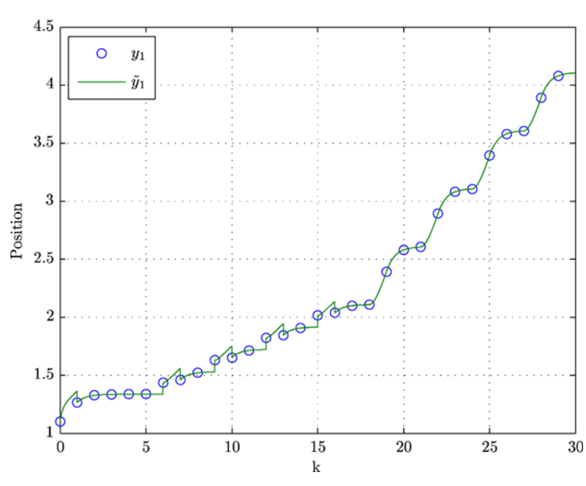

Fig. 2 Simulated and measured position of automobile

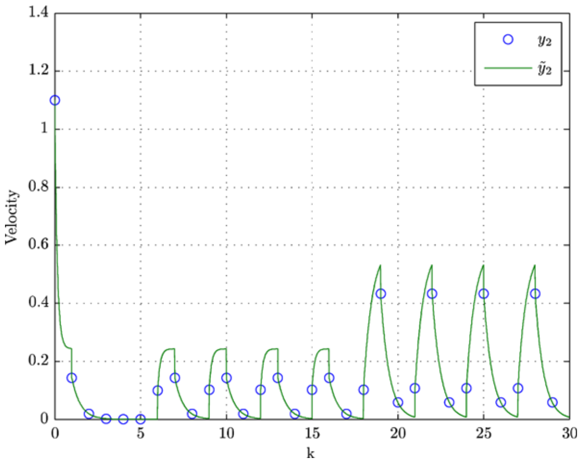

Fig. 3 Simulated and measured velocity of automobile

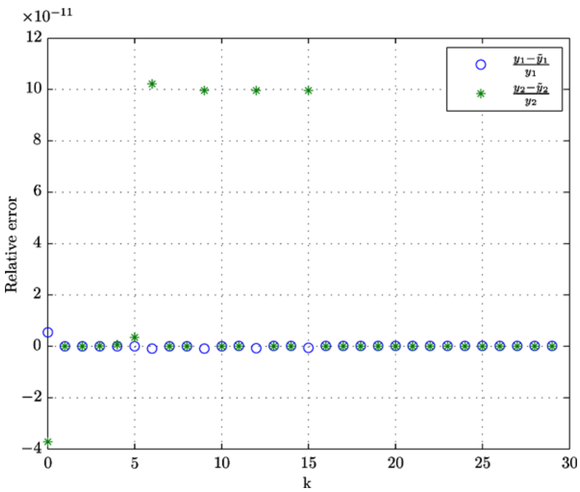

Fig. 4 Relative error of outputs

gular values of the Hankel matrix are

$$\Sigma_1 = \mathrm{diag}\left[3.9807 \quad 0.1183 \quad 1.9678 \times 10^{-16}\right] \quad (69)$$

implying that the order of the system is $n = 2$. Using the identified system with the identified initial condition $\tilde{x}(0) = [-2.2920 \; 1.0197]^T$ to perform numerical simulations with the same input sequence shown in Fig. 1, the simulated outputs $\tilde{y}_1$ and $\tilde{y}_2$ comparing to the measured (actual) outputs y_1 and y_2 are shown in Figs. 2 and 3, and the relative errors are plotted in Fig. 4.

4.2 Induction motor

The bilinear model of induction motor drives is given by a fourth-order differential equation [26], which can be expressed in the form of (2). The state and control variables are

$$x = [\,\phi_{ds} \quad \phi_{qs} \quad i_{ds} \quad i_{qs}\,]^T, \qquad u = [\,v_{ds} \quad v_{qs} \quad \omega_s\,]^T \quad (70)$$

where ϕ_{ds} and ϕ_{qs} are projections of the stator flux, i_{ds} and i_{qs} are projections of the stator current, v_{ds} and v_{qs} are projections of the supply voltage, ω_s is the slip angular frequency. The system matrices are given by

$$A_c = \begin{bmatrix} 0 & 321.57 & -0.312 & 0 \\ -312.57 & 0 & 0 & -0.312 \\ 98.87 & 27059 & -44.93 & 2.57 \\ -27059 & 98.87 & -2.57 & -44.93 \end{bmatrix},$$

$$B_c = \begin{bmatrix} 1 & 0 & 0 \\ 0 & 1 & -7.3 \\ 87.3 & 0 & 87.8 \\ 0 & 87.3 & -53 \end{bmatrix}, \quad (71)$$

$$N_{c1} = \begin{bmatrix} 0 & 0 & 0 & 0 \\ 0 & 0 & 0 & 0 \\ 0 & 0 & 0 & 0 \\ 0 & 0 & 0 & 0 \end{bmatrix}, \qquad N_{c2} = \begin{bmatrix} 0 & 0 & 0 & 0 \\ 0 & 0 & 0 & 0 \\ 0 & 0 & 0 & 0 \\ 0 & 0 & 1 & 0 \end{bmatrix},$$

$$N_{c3} = \begin{bmatrix} 0 & 1 & 0 & 0 \\ -1 & 0 & 0 & 0 \\ 0 & 0 & 0 & 1 \\ 0 & 0 & 0 & 0 \end{bmatrix},$$

and the initial condition is $x(0) = [-0.07 \; 0.04 \; 15 \; 47]^T$. Assume that the system matrices of the measurement equation (4) are

$$C = \begin{bmatrix} 1 & 0 & 0 & 0 \\ 0 & 1 & 0 & 0 \\ 0 & 0 & 1 & 0 \\ 0 & 0 & 0 & 1 \end{bmatrix}, \qquad D = \begin{bmatrix} 0 & 0 & 0 \\ 0 & 0 & 0 \\ 0 & 0 & 0 \\ 0 & 0 & 0 \end{bmatrix}. \quad (72)$$

The first step is to design an input sequence for excitation of the bilinear system. Let the control inputs be given as

$$W = \begin{bmatrix} 1 & 0 & 0 \\ 1 & 1 & 0 \\ 1 & 0 & 1 \end{bmatrix}, \quad (73)$$

and $\alpha = 2$, $\beta = p = 4$ with the sampling time $\Delta t = 0.005$. Figure 5 shows the input sequence where the quantities u_1, u_2, and u_3 are the sampled input values at the designated application points, and the quantities $\tilde{u}_1$, $\tilde{u}_2$, and $\tilde{u}_3$ are the pulses used in the excitation process. The first pulse vector includes all three inputs, whereas the second and third pulse vectors contain only the second and third inputs, respectively. The first pulse applied at $k = 0$ generates five ($\alpha + \beta - 1 = 5$) free-decay response data that are used to identify the state matrix A_c, the output matrix C, and the observability matrix U_1. The remaining pulses at $k = 6, 8, 10, \ldots,$ produce only one ($\alpha - 1 = 1$) free-decay response data each. The resulting pulse responses shown in Figs. 6 to 10 show a clear response decaying during the free-decay periods. These remaining pulse responses are used to identify the remaining system matrices N_c, B_c, and D.

Using the SEMP method, we obtain the identified initial condition

$$\tilde{x}(0) = [-67.1845 \; -6.0376 \; -3.5100 \; -5.1913]^T,$$

and the system matrices $\tilde{A}_c$, $\tilde{B}_c$, $\tilde{C}$, and $\tilde{D}$:

$$\begin{aligned}
\tilde{A}_c &= \begin{bmatrix} -22.2743 & 251.3680 & 72.0502 & -184.9701 \\ -1.7703 & 21.8923 & -434.6409 & 39.6915 \\ -4.8607 & 262.9303 & -62.8138 & -180.2745 \\ -3.2837 & 26.4862 & -66.7765 & -26.6643 \end{bmatrix}, \\
\tilde{B}_c &= \begin{bmatrix} 13.8085 & -77.3616 & 170.8562 \\ 99.5447 & 45.5043 & 606.6941 \\ 47.6701 & -68.3619 & -449.0471 \\ 18.5967 & -2.5111 & 440.6662 \end{bmatrix}, \\
\tilde{C} &= \begin{bmatrix} 0.0005 & 0.0086 & 0.0054 & -0.0065 \\ -0.0004 & 0.0054 & -0.0105 & -0.0014 \\ -0.3331 & 0.5199 & 0.7107 & 0.3368 \\ -0.6689 & 0.3367 & -0.2738 & -0.6035 \end{bmatrix}, \\
\tilde{D} &= \begin{bmatrix} 0.0011 & -0.0008 & -0.0007 \\ 0.0056 & -0.0045 & -0.0039 \\ 0.5754 & -0.4448 & -0.3914 \\ 0.3295 & -0.2713 & -0.2307 \end{bmatrix} \times 10^{-11},
\end{aligned} \tag{74}$$

and the bilinearity matrices $\tilde{N}_{c1}$, $\tilde{N}_{c2}$, and $\tilde{N}_{c3}$

$$\begin{aligned}
\tilde{N}_{c1} &= \begin{bmatrix} 0.0001 & -0.0007 & 0.0142 & -0.0262 \\ 0.0005 & -0.0770 & -0.1078 & 0.1137 \\ -0.0002 & -0.1147 & -0.0888 & 0.1024 \\ -0.0002 & -0.1183 & -0.0956 & 0.1404 \end{bmatrix} \\
&\quad \times 10^{-8}, \\
\tilde{N}_{c2} &= \begin{bmatrix} 0.3817 & -0.5957 & -0.8142 & -0.3859 \\ 0.1064 & -0.1660 & -0.2270 & -0.1076 \\ 0.0150 & -0.0235 & -0.0321 & -0.0152 \\ 0.1815 & -0.2833 & -0.3873 & -0.1835 \end{bmatrix}, \\
\tilde{N}_{c3} &= \begin{bmatrix} 0.3808 & -0.0382 & -0.6742 & 0.4320 \\ -0.4672 & -0.1786 & -1.0480 & 0.0433 \\ -0.1240 & 0.7817 & -0.0150 & -0.5896 \\ -0.6264 & -0.4120 & 0.1695 & -0.1872 \end{bmatrix}.
\end{aligned} \tag{75}$$

The maximum difference of eigenvalues of A_c and N_{ci}'s between the original and identified system is 1.2544×10^{-5}, and so the identified system matrices are similar to the original ones. Using the identified initial state and system matrices with the same input sequence shown in Fig. 5 to perform numerical simulations, the simulated outputs $\tilde{y}_1$, $\tilde{y}_2$, and $\tilde{y}_3$ and the

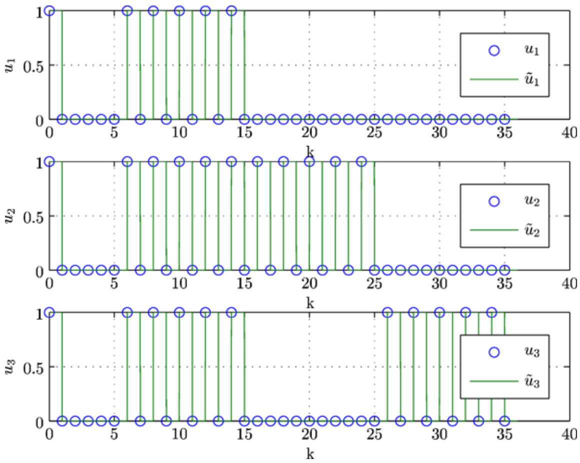

Fig. 5 Sampled and pulse input sequence

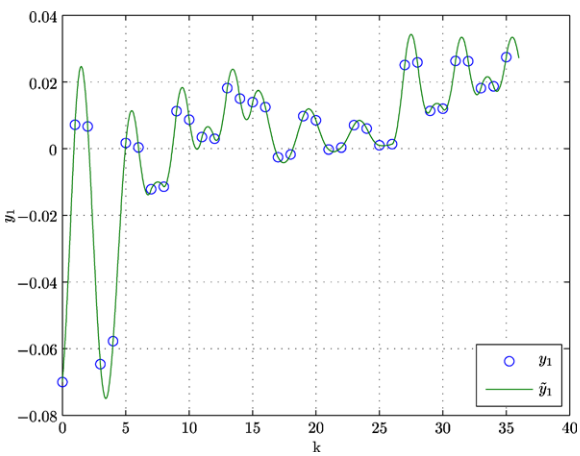

Fig. 6 Simulated and measured ϕ_{ds}

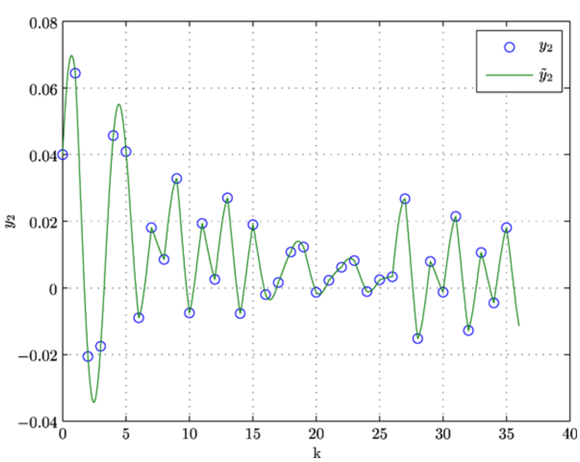

Fig. 7 Simulated and measured ϕ_{qs}

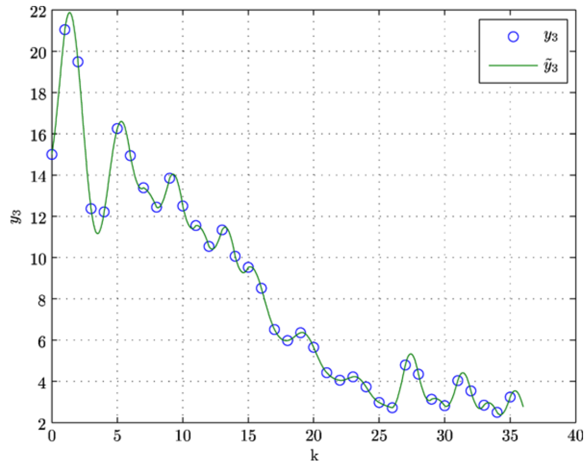

Fig. 8 Simulated and measured i_{ds}

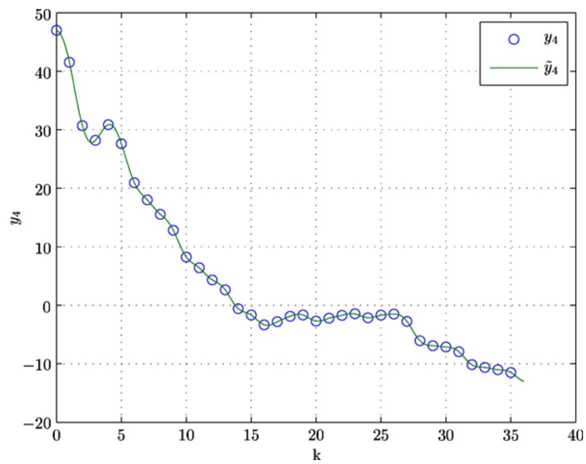

Fig. 9 Simulated and measured i_{qs}

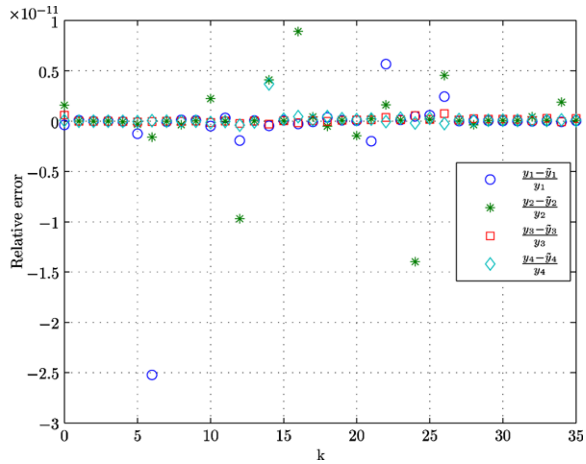

Fig. 10 Relative error of outputs

measured (actual) outputs y_1, y_2, and y_3 are shown in Figs. 6 to 9, and the relative errors are plotted in Fig. 10. These simulation results demonstrate good correspondence between the identified and actual output responses.

5 Concluding remarks

We have presented an identification process for determination of a continuous-time bilinear model using a single experiment with a sequence of pulse inputs and free decay. The period of free decay between pulses depends on the size of Hankel matrix for determination of the system matrices describing the linear portion of a bilinear system. Experiments may be performed continuously with multiple inputs simultaneously, but waiting time is not required for the system to decay completely as the multiple experiments do. The identification method can be started anytime due to the capability of identifying system initial condition that makes it appropriate for real-time/on-line applications.

Simulation results illustrate the validity of the proposed method for identification of a continuous-time bilinear system. Simulation studies have also revealed that a valid choice of pulse and free-decay responses is important for the identification results. Some directions of continued research can be addressed in the future. One study is to extend the identification method to a general class of observable and reachable bilinear systems such as removing the observability requirement for the linear part of the bilinear systems. Another study is the further investigations of proper choice of input signals.

References

1. Juang, J.-N.: Applied System Identification. Prentice Hall, New Jersey (1994)
2. Juang, J.-N., Phan, M.Q.: Identification and Control of Mechanical Systems. Cambridge University Press, New York (2001)
3. Rugh, W.J.: Nonlinear System Theory: The Volterra/Wiener Approach. The John Hopkins University Press, Baltimore (1981). ISBN 0-8018-2549-0
4. Svoronos, S., Stephanopoulos, G., Aris, R.: Bilinear approximation of general non-linear dynamic systems with linear inputs. Int. J. Control **31**(1), 109–126 (1980)
5. Lo, J.T.-H.: Global bilinearization of systems with control appearing linearly. SIAM J. Control **13**(4), 879–885 (1975)
6. Bruni, C., DiPillo, G., Koch, G.: On the mathematical models of bilinear systems. Ric. Autom. **2**(1), 11–26 (1971)
7. Bruni, C., DiPillo, G., Koch, G.: Bilinear systems: An appealing class of nearly linear systems in theory and application. IEEE Trans. Autom. Control **AC-19**, 334–348 (1974)
8. Mohler, R.R., Kolodziej, W.J.: An overview of bilinear system theory and applications. IEEE Trans. Syst. Man Cybern. **SMC-10**, 683–688 (1980)
9. Elliott, D.L.: Bilinear systems. In: Webster, J. (ed.) Encyclopedia of Electrical Engineering, vol. II, pp. 308–323. Wiley, New York (1999)
10. Mohler, R.R.: Nonlinear Systems. Applications to Bilinear Control, vol. II. Prentice-Hall, New Jersey (1991)
11. Paraskevopoulos, P., Tsirikos, A., Arvanitis, K.: A new orthogonal series approach to state space analysis of bilinear systems. IEEE Trans. Autom. Control **39**, 793–797 (1994)
12. Karanam, V.R., Frick, P.A., Mohler, R.R.: Bilinear system identification by Walsh functions. IEEE Trans. Autom. Control **23**, 709–713 (1973)
13. Jha, A.N., Saxena, A.S., Rajamani, V.S.: Parameter estimation algorithms for bilinear and non-linear systems using Walsh functions: Recursive approach. Int. J. Syst. Sci. **23**, 283–290 (1992)
14. Cheng, B., Hsu, N.-S.: Analysis and parameter estimation of bilinear systems via block-pulse functions. Int. J. Control **36**, 53–65 (1982)
15. Dai, H., Sinha, N.K.: Robust identification of systems using block-pulse functions. IEE Proc. Part D. Control Theory Appl. **139**, 308–316 (1992)
16. Liu, C.C., Shih, Y.P.: Analysis and parameter estimation of bilinear systems via Chebyshev polynomials. J. Franklin Inst. **317**, 373–382 (1984)
17. Hwang, C., Chen, M.Y.: Analysis and parameter identification of bilinear systems via shifted Legendre polynomials. Int. J. Control **44**, 351–362 (1986)
18. Daniel-Berhe, S., Unbehauen, H.: Bilinear continuous-time systems identification via Hartley-based modulating functions. Automatica **34**, 499–503 (1998)
19. Daniel-Berhe, S., Unbehauen, H.: State space identification of bilinear continuous-time canonical systems via batch scheme Hartley modulating functions approach. In: Proceedings of the 37th IEEE Conference on Decision and Control, Tampa, FL, pp. 4482–4487, December (1998)
20. Karray, F., Dwyer, T.A.W. III: On the nonlinear system identification of a class of bilinear dynamical models. In: Proceedings of the 30th IEEE Conference on Decision and Control, Brighton, UK, vol. 1, pp. 778–782 (1991)
21. Karray, F., Dwyer, T., Makrakis, D.: Bilinear approximation and identification for nonlinear system modeling. In: Proceedings of the 35th IEEE Conference on Decision and Control, Kobe, Japan, vol. 1, pp. 1088–1093 (1996)
22. Juang, J.-N.: Continuous-time bilinear system identification. Nonlinear Dyn. **39**(1–2), 79–94 (2005)
23. Phan, M.Q., Celik, H.: A superspace method for discrete-time bilinear model identification by interaction matrices, Paper AAS 10-330. In: Proceedings of the Kyle T. Alfriend Astrodynamics Symposium, Monterey, CA, May (2010)
24. Ekman, M., Larson, E.K.: Parameter estimation of continuous-time bilinear systems based on numerical integration and separable non-linear least-squares. Int. J. Control **80**(3), 329–339 (2007)

25. Sontag, E.D., Wang, Y., Megretski, A.: Input classes for identification of bilinear systems. IEEE Trans. Autom. Control **54**, 195–207 (2009)
26. Aganović, Z., Gajić, Z.: Linear Optimal Control of Bilinear Systems. Lecture Notes in Control and Information Sciences, vol. 206. Springer, London (1995)